Measurements of the wave–front outer scale at Paranal : influence of this parameter in interferometry

R. Conan[a], A. Ziad[a], J. Borgnino[a], F.Martin[a] and A. Tokovinin[b]

[a]U.M.R. 6525 Astrophysique, Université de Nice–Sophia–Antipolis, F–06108 Nice Cedex 2, France
[b]Sternberg Astronomical Institute, Universitestsky prosp., 13, 119899 Moscow, Russia

ABSTRACT

The Generalized Seeing Monitor (GSM) has undertaken a campaign of measurement of the optical turbulent parameters : the Fried's parameter, the outer scale ($\mathcal{L}_0$) and the isoplanatic patch, at Paranal, the site of the VLT, in December 1998. The principle aim of this mission was to measure $\mathcal{L}_0$ values at Paranal. In a first part, we present the GSM, the results of the mission and particularly the statistics of $\mathcal{L}_0$. In a second part, we emphasize the effect of $\mathcal{L}_0$ on the optical path difference (OPD) values for the co–phasing of an interferometer. We derive the exact formulation of the OPD for the Von Kármán model and we give the expected OPD at Paranal with $\mathcal{L}_0$ values measured by the GSM. We give also the expression of the residual OPD at the output of a fringe tracker system as a function of $\mathcal{L}_0$, of the exposure time of the fringe sensor and of the frequency of the closed–loop of the system.

Keywords: site testing, outer scale, atmospheric turbulence, interferometry, co–phasing

1. INTRODUCTION

1.1. The GSM instrument

The Generalized Seeing Monitor (GSM)[1,2] is a monitor of the optical turbulent parameters (OTP) : the Fried's parameter r_0, the spatial coherence outer scale of the wave front $\mathcal{L}_0$ and the isoplanatic patch θ_0. All are calculated for a wavelength $\lambda = 500$ nm. It measures one component of the gradient of the wave front (the angle–of–arrival fluctuations) simultaneously at four points. It is constituted of four telescopes (Ref. 1 fig.1) with 10 cm of pupil diameter. Two of them are supported by the same equatorial mount in order to be able to work in a differential mode to measure the r_0 without beeing corrupted by vibrations. Both telescopes on the same mount are 0.25 m apart, 1 m in the East direction is the second one and the third one is 0.8 m in the South direction. This layout gives 6 baselines and so 6 cross–correlations used for the determination of the $\mathcal{L}_0$. A standard automatic acquisition of the AA progresses as it follows : first, with an exposure time of 5 ms, the AA are measured every 5 ms during 2 mn, then, the acquisition process is interrupted for 2 mn of data processing leading to the computation of the r_0, $\mathcal{L}_0$ and θ_0 and the acquisition process is re–launched.

1.2. The campaign of measurement at Paranal

The measurements started up the November 27 1998 and ceased the December 20 1998. The campaign is divided in two sets of continuous nights from the November 27 to the December 08 and from the 14 to the 20 of December. The median values, over the whole mission, of the seeing ε, $\mathcal{L}_0$ and θ_0 are respectively 0.9 arcsec, 22 m and 1.9 arcsecond. Due to the particularly clear nights at Paranal without any clouds, this campaign was the most fruitful of all the GSM missions with an average of 6h30mn of effective measurement time per night and a total of 1884 measurements of each parameter shared among the 19 nights of the missions.

Correspondence to R. Conan: E–mail: Rodolphe.CONAN@unice.fr

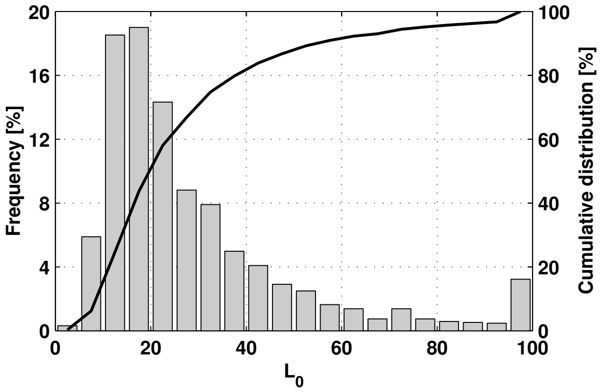

Figure 1. Histogram of $\mathcal{L}_0$ values. The $\mathcal{L}_0$ values larger than 100 m are not taken into account in the histogram since they represent less than 3% of the whole data.

1.3. The outer scale measured at Paranal

The $\mathcal{L}_0$ values are deduced from the spatial covariances of the AA fluctuations. The layout of the four telescopes of the GSM permits the computation of 6 covariances. These covariances are normalized by the structure function computed from the AA measured by both telescopes on the differential mount. This structure function is not affected by vibrations. The covariances are also not affected by vibrations, wind shake effects or tracking errors since it has been checked that the noises from each telescope are uncorrelated. Therefore, the normalized covariances depend only on the $\mathcal{L}_0$. The best fit of the experimental normalized covariances by theoretical ones gives the $\mathcal{L}_0$ value. The theoretical normalized covariances have been computed from the spectrum of the wave–front phase fluctuations for the Von Kármán[3–6] model:

$$W_\varphi(f) = 0.0229 r_0^{-5/3}\left(f^2 + \left(\frac{1}{\mathcal{L}_0}\right)^2\right)^{-11/6}, \tag{1}$$

where f is the spatial frequency and $0.0229 = \dfrac{\Gamma^2(11/6)}{2\pi^{11/3}}\left[\dfrac{24}{5}\Gamma(6/5)\right]^{5/6}$.

The statistic of the $\mathcal{L}_0$ at Paranal[7] contains 1884 values. It follows a log–normal distribution (Fig. 1) with a mean value equal to 24 m and 68% of the values of the distribution of $\log(\mathcal{L}_0)$ lies between 15 m and 37 m. One has noted, for several nights, some periods of great stability of $\mathcal{L}_0$ values associated with low values (typically around 15 m) leading to the lowest night average values ever measured by the GSM. Two nights gave uncommon high values ($\sim$ 45 m). During these nights the wind blown from the South which is a non–typical situation for the Paranal. As already mentioned during previous campaigns of the GSM,[8,1,2,9] bursts of $\mathcal{L}_0$ values were noticed. And as for other sites, no effective correlation between r_0 and $\mathcal{L}_0$ values has been underscored.

2. CO–PHASING AND WAVE–FRONT OUTER SCALE

2.1. The Optical Path Difference

2.1.1. Theory

The randomly fluctuations of the optical path difference (OPD), due to the propagation of light beams into the atmosphere, between two telescopes separated by a distance B is a fundamental limitations to performances of interferometers.

The variance of the OPD between two points is given by

$$\sigma^2_{OPD} = \left(\frac{\lambda}{2\pi}\right)^2 \langle|\varphi(\vec{r}) - \varphi(\vec{r}+\vec{B})|^2\rangle, \tag{2}$$

where $\varphi(\vec{r})$ is the phase of the wave front and $\vec{B}$ is the baseline vector. Since $\langle|\varphi(\vec{r}) - \varphi(\vec{r}+\vec{B})|^2\rangle$ is the well–known structure function of phase fluctuations $\mathcal{D}_\varphi(\vec{B})$ (or differential phase variance), the standard deviation of the OPD is

$$\sigma_{OPD} = \frac{\lambda}{2\pi}\sqrt{\mathcal{D}_\varphi(\vec{B})}. \tag{3}$$

In the rest of the paper, all the calculus will be made for $\mathcal{D}_\varphi(\vec{B})$ as Eq. (3) gives straightforwardly the corresponding σ_{OPD}. In the framework of the Kolmogorov model[10,11] , the expression of $\mathcal{D}_\varphi(\vec{B})$ is

$$\mathcal{D}_\varphi(B) = 6.88\left(\frac{B}{r_0}\right)^{5/3}. \tag{4}$$

But Equation (4) diverges when B tends towards infinity as it is valid only in the inertial range, i.e. when B values lie between the inner and outer scale values (from few centimeters to few ten of meters).

For large baselines (close to of larger than the outer scale), $\mathcal{D}_\varphi(\vec{B})$ is expected to saturate, which lead to an attenuation of the spectrum of the phase fluctuations in low frequencies regime as for the spectrum of the Von Kármán model.

$\mathcal{D}_\varphi(\vec{B})$ is deduced from the phase spectrum $W_\varphi(f)$ by the relation

$$\mathcal{D}_\varphi(B) = 4\pi\int_0^{+\infty} f W_\varphi(f)[1 - J_0(2\pi B f)]df. \tag{5}$$

Putting Equation (1) into Equation (5) and performing the integration give the following expression of the structure function[12–14] in the framework of the Von Kármán model

$$\mathcal{D}_\varphi(B) = 0.1717\left(\frac{r_0}{\mathcal{L}_0}\right)^{-5/3}\left[1.0056 - \left(\frac{2\pi B}{\mathcal{L}_0}\right)^{5/6} K_{5/6}\left(\frac{2\pi B}{\mathcal{L}_0}\right)\right] \tag{6}$$

where $K_{5/6}(x)$ is the Mac–Donald function, $0.1717 = \frac{2^{1/6}\Gamma(11/6)}{\pi^{8/3}}\left[\frac{24}{5}\Gamma\left(\frac{6}{5}\right)\right]$ and $1.0056 = \frac{\Gamma(5/6)}{2^{1/6}}$. Equation (6) is valid for all baselines larger than the inner scale and when the pupil diameter D of the telescope is much smaller than the correlation scale of the phase fluctuations.

Taking into account the finite size D of the pupil permits to rewrite Equation (5) in a more general formulation

$$\mathcal{D}_\varphi(B) = 4\pi\int_0^{+\infty} f W_\varphi(f)[1 - J_0(2\pi B f)]\left[\frac{2J_1(\pi D f)}{\pi D f}\right]^2 df. \tag{7}$$

The solution of Equation (7) can be divided into three regimes:

1. $D < B < \frac{\mathcal{L}_0}{\pi}$,
2. $D < \frac{\mathcal{L}_0}{\pi} < B$,
3. $\frac{\mathcal{L}_0}{\pi} < D < B$.

For cases 1 and 2, Equation (7) is expanded in series[15] with fast convergence and for the last case, an asymptotic solution is given.

1. $D < B < \frac{\mathcal{L}_0}{\pi}$:

$$\begin{aligned}\mathcal{D}_\varphi(B) \quad &= -\frac{4\Gamma(11/6)}{\pi^{3/2}}\left[\frac{24}{5}\Gamma(6/5)\right]^{5/6}\left(\frac{B}{r_0}\right)^{5/3}\times \\ &\left\{\sum_{n=1}^{+\infty}\sum_{m=0}^{+\infty}\frac{(-1)^n}{n!}\frac{(-1)^m}{m!}(\pi B f_0)^{2n-5/3}(\pi D f_0)^{2m}\Gamma\left[\begin{array}{c} n+m+1, 5/6-n-m, m+3/2 \\ n+1, m+3, m+2\end{array}\right]\right. \\ &\left.+\sum_{n=0}^{+\infty}\sum_{m=0}^{+\infty}\frac{(-1)^n}{n!}\frac{(-1)^m}{m!}(\pi B f_0)^{2n}\left(\frac{D}{B}\right)^{2m}\Gamma\left[\begin{array}{c} m-n-5/6, n+11/6, m+3/2 \\ n-m+11/6, m+3, m+2\end{array}\right]\right\}\end{aligned} \tag{8}$$

2. $D < \frac{\mathcal{L}_0}{\pi} < B$:

$$\begin{aligned}
\mathcal{D}_\varphi(B) &= \frac{4\Gamma(11/6)}{\pi^{7/3}} \left[\frac{24}{5}\Gamma(6/5)\right]^{5/6} \\
&\times \left\{ \pi^{-5/6}(r_0 f_0)^{-5/3} \sum_{n=0}^{+\infty} \frac{(-1)^n}{n!} (\pi D f_0)^{2n} \Gamma \left[\begin{array}{c} n+1, 5/6-n, n+3/2 \\ n+3, n+2 \end{array} \right] \right. \\
&\left. - \left(\frac{B}{r_0}\right)^{5/3} (B f_0)^{-4/3} \exp(-2\pi B f_0) \sum_{n=0}^{+\infty} \frac{(-1)^n}{n!} (\pi D f_0)^{2n} \Gamma \left[\begin{array}{c} n+3/2 \\ n+3, n+2 \end{array} \right] \right\}
\end{aligned} \tag{9}$$

3. $\frac{\mathcal{L}_0}{\pi} < D < B$:

$$\mathcal{D}_\varphi(B) = \frac{4\Gamma^2(11/6)}{\pi^{14/3}} \left[\frac{24}{5}\Gamma(6/5)\right]^{5/6} \left(\frac{D}{r_0}\right)^{5/3} (D f_0)^{-11/3} \tag{10}$$

where $f_0 = \dfrac{1}{\mathcal{L}_0}$.

Asymptotic solutions for Eqs. (8) and (9) are found in expanding each sum with the first values of n and m. The asymptotic solutions for the different regimes are summarized below:

1. $D < B \ll \frac{\mathcal{L}_0}{\pi}$:

$$\mathcal{D}_\varphi(B) = 6.88 \left(\frac{B}{r_0}\right)^{5/3} \left[1 - 1.49 \left(\frac{B}{\mathcal{L}_0}\right)^{1/3}\right], \tag{11}$$

2. $D \ll \frac{\mathcal{L}_0}{\pi} \ll B$:

$$\mathcal{D}_\varphi(B) = 0.17 \left(\frac{\mathcal{L}_0}{r_0}\right)^{5/3}, \tag{12}$$

3. $\frac{\mathcal{L}_0}{\pi} \ll D < B$:

$$\mathcal{D}_\varphi(B) = 0.06 \left(\frac{D}{r_0}\right)^{5/3} \left(\frac{D}{\mathcal{L}_0}\right)^{-11/3}. \tag{13}$$

Equation (11) tends towards Equation (4) when $\mathcal{L}_0$ goes to infinity as B falls in the inertial range. Equation (12) shows that when the $\mathcal{L}_0$ is much larger than D but much lower than B, the structure function and so the standard deviation of the OPD are independent of both the pupil diameter and the baseline. This noteworthy property had been already underscored by Mariotti (Ref. 16). For $\mathcal{L}_0$ values small compared to B and D values, $\mathcal{D}_\varphi(B)$ and σ_{OPD} are functions of the ratios D/r_0 and $D/\mathcal{L}_0$ but are independent of the baseline values.

The last three equations show that when baseline values are larger than $\mathcal{L}_0$ values, we can expect than the OPD will not vary notably from one baseline to another one as the saturation of $\mathcal{D}_\varphi(B)$ is reached. This is put in evidence in Figs. 2 and 3. Figure 2 shows structure functions plotted as functions of the baseline B. They are computed from Equation (6) for $\mathcal{L}_0$= 25 m (dashed line), from Equation (4) for $\mathcal{L}_0$= ∞ (dashed–dotted line) and from Equation (7) for D = 1, 5 and 10 m and $\mathcal{L}_0$= 25 m. When $B > \mathcal{L}_0$, structure functions grow asymptotically towards the saturation level. In Figure 3, σ_{OPD} is computed versus B and $\mathcal{L}_0$ for D = 10 m and r_0 = 10 cm and the isolines (full lines) are displayed. The label of each isoline gives the value of σ_{OPD} in wavelength unit. The first diagonal which corresponds to the case $B = \mathcal{L}_0$ is also drawn (dashed line). As previously, for a fixed $\mathcal{L}_0$, σ_{OPD} does not vary noticeably when B becomes larger than $\mathcal{L}_0$.

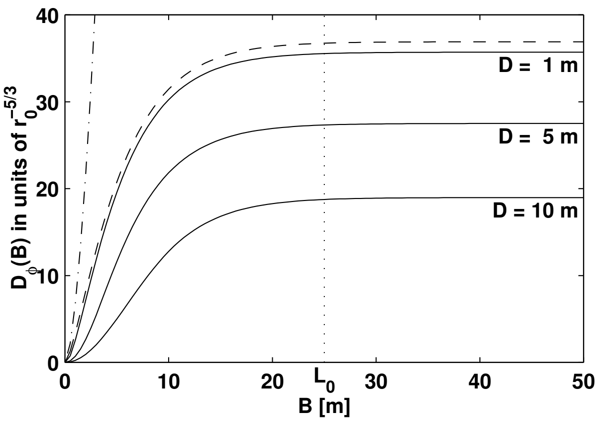

Figure 2. Structure function of the phase fluctuations in units of $r_0^{-5/3}$ computed from Equation (6) for $\mathcal{L}_0$= 25 m (dashed line) and for $\mathcal{L}_0$= ∞ (dashed–dotted line) and from Equation (7) for D = 1,5 and 10 m and $\mathcal{L}_0$= 25 m (full lines).

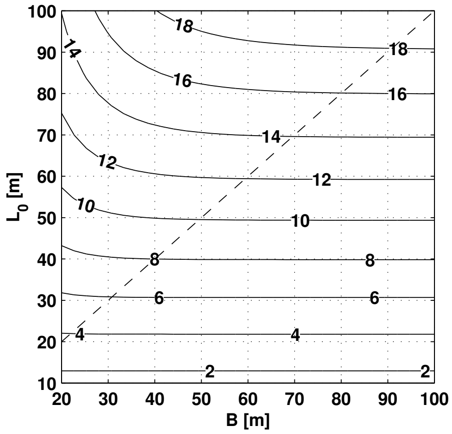

Figure 3. Isoline of the standard deviation of the OPD in units of wavelength as a function of B and $\mathcal{L}_0$ for D = 10 m and r0 = 10 cm.

2.1.2. Experimental results

Assuming the validity of the Von Kármán spectrum to modelize the structure function of the phase out of the inertial range, we can deduce the expected OPD at Paranal during the campaign of the GSM. Computing Equation (1) with all the couples $(r_0; \mathcal{L}_0)$ measured by the GSM at Paranal and putting them into Equation (7) and performing the integral for baselines 40, 100 and 200 m with D = 8.2 m lead to the values of σ_{OPD} using Equation (3).

Figure 4 shows the histograms of σ_{OPD} calculated in this way in the framework of the Kolmogorov model (a) and of the Von Kármán model (b). σ_{OPD} is given in wavelength unit. The comparison of the OPD statistics between both models shows than the OPD is reduced by a factor 10 when $\mathcal{L}_0$ values are taken into account. Moreover, as 80% of the $\mathcal{L}_0$ values are lower than the smallest baseline ($B = 40$ m) (see Fig. 1), the OPD with finite $\mathcal{L}_0$ is almost insensible to baseline variations.

2.2. OPD residual after correction by a fringe tracker

In the previous section, we have shown how if we estimate the OPD holding into account the finite size of the outer scale, OPD values are considerably reduced compared to those given for an infinite outer scale. However, the remaining OPD due to random atmospheric phase fluctuations have to be compensated to attenuate the blurring of long exposure interferograms in order to obtain sufficiently accurate measurements of the fringes visibility.

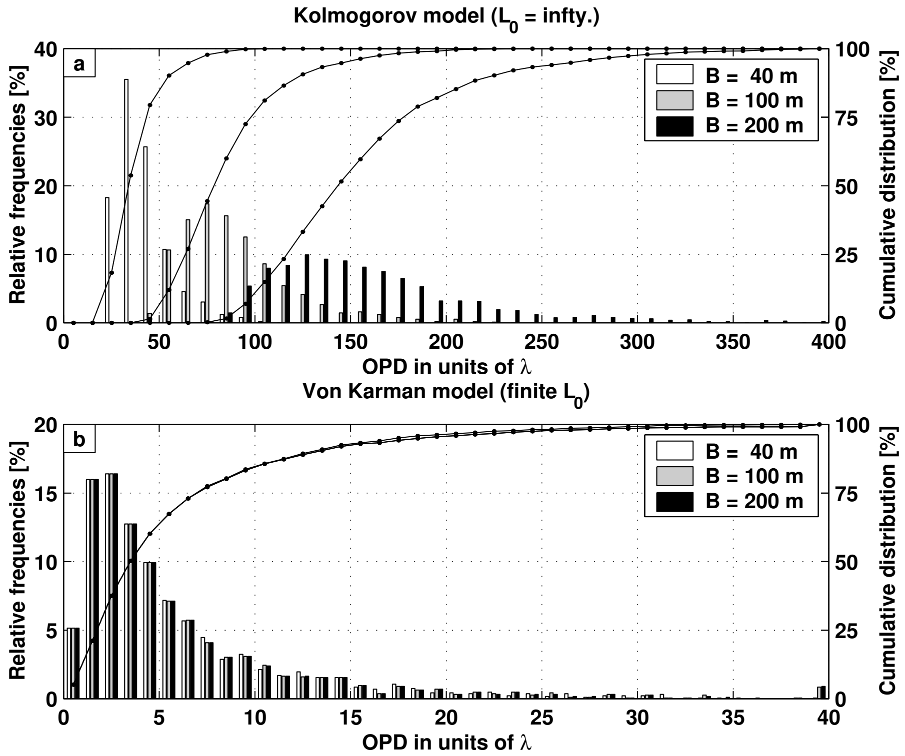

Figure 4. Histograms of the standard deviation of the OPD in units of wavelength for the Kolmogorov model (a) and for the Von Kármán model (b) for baselines B = 40,100 and 200 m, for a aperture diameter D = 8.2 m and for all the values of r_0 and $\mathcal{L}_0$ measured by the GSM at Paranal.

In this aim, interferometers[17–20] are all equipped with a fringe tracker system, a simplified sketch of which is given in Figure 5 for a two apertures interferometer. A fringe tracker system is composed of a fringe sensor, a servo–control and a fast delay line (FDL). The fringe sensor measures the difference $\Delta\varphi$ between the averaged phase of each aperture, this phase difference is transmitted to the servo–control which converts $\Delta\varphi$ into OPD and drives the FDL to add $\Delta\varphi$ to one of the incoming phase.

The residual phase difference $\Delta\varphi_r$ at the output of the fringe tracker is

$$\Delta\varphi_r = \varphi(\vec{r}+\vec{B},t) + \Delta\varphi - \varphi(\vec{r},t)\ , \tag{14}$$

and its variance is

$$\sigma^2_{\Delta\varphi_r} = \left\langle \left|\varphi(\vec{r}+\vec{B},t) + \Delta\varphi - \varphi(\vec{r},t)\right|^2 \right\rangle = \mathcal{D}_{\varphi_r}(\vec{B})\ , \tag{15}$$

which is equal to the structure function $\mathcal{D}_{\varphi_r}(\vec{B})$ of the residual phase.

Among the different errors susceptible to affect the measurement of $\Delta\varphi$, we consider only the effects of the finite exposure time T of the fringe sensor and the finite response time τ of the servo–control which is the the time difference between the date of the measurement of $\Delta\varphi$ and the date of the corresponding compensation introduced by the FDL. With these two errors, $\Delta\varphi$ can be written

$$\Delta\varphi = \varphi_T(\vec{r}+\vec{B},t+\tau) - \varphi_T(\vec{r},t+\tau)\ , \tag{16}$$

where

$$\varphi_T(\vec{r},t+\tau) = \frac{1}{T}\int_{-\infty}^{+\infty} dt'\,\Pi\left(\frac{(t+\tau)-t'}{T}\right)\varphi(\vec{r},t')\ . \tag{17}$$

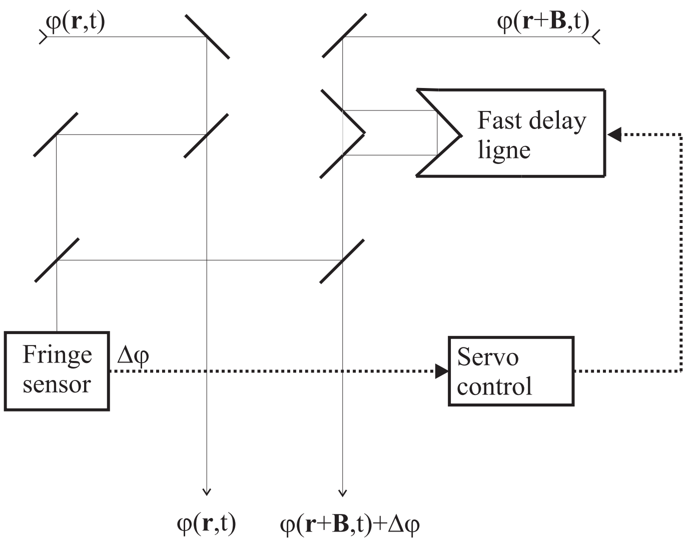

Figure 5. Simplified sketch of a fringe tracker system.

$\Pi(t)$ is the rectangle function[21]:

$$\Pi\left(\frac{t}{T}\right) = 1, \text{ if } \left|\frac{\mathrm{t}}{\mathrm{T}}\right| \leq \frac{1}{2}$$
$$= 0, \text{ otherwise.} \tag{18}$$

Putting Equation (16) into Equation (15), we obtain :

$$\mathcal{D}_{\varphi_r}(\vec{B}) = \left\langle \left| \left(\varphi(\vec{r},t) - \varphi(\vec{r}+\vec{B},t)\right) - \left(\varphi_T(\vec{r},t+\tau) - \varphi_T(\vec{r}+\vec{B},t+\tau)\right) \right|^2 \right\rangle, \tag{19}$$

$$= \left\langle \left| \left(\varphi(\vec{r},t) - \varphi(\vec{r}+\vec{B},t)\right) \right|^2 \right\rangle + \left\langle \left| \left(\varphi_T(\vec{r},t+\tau) - \varphi_T(\vec{r}+\vec{B},t+\tau)\right) \right|^2 \right\rangle - 2\left\langle \left| \left(\varphi(\vec{r},t) - \varphi(\vec{r}+\vec{B},t)\right) \left(\varphi_T(\vec{r},t+\tau) - \varphi_T(\vec{r}+\vec{B},t+\tau)\right) \right| \right\rangle \tag{20}$$

The two first terms are respectively the structure function $\mathcal{D}_\varphi(\vec{r},t)$ of the instantaneous phase and the structure function $\mathcal{D}_{\varphi_T}(\vec{r},t)$ of the phase averaged for an exposure time T and the last term is a coupling term $\mathcal{C}_\varphi(\vec{B},T,\tau)$ between the instantaneous phase and the averaged phase.

$$\mathcal{D}_{\varphi_r}(\vec{B}) = \mathcal{D}_\varphi(\vec{B}) + \mathcal{D}_{\varphi_T}(\vec{B}) - 2\mathcal{C}_\varphi(\vec{B},T,\tau) \tag{21}$$

where

$$\mathcal{C}_\varphi(\vec{B},T,\tau) = 2\left[\langle\varphi(\vec{r},t)\varphi_T(\vec{r},t+\tau)\rangle - \langle\varphi(\vec{r},t)\varphi_T(\vec{r}+\vec{B},t+\tau)\rangle\right] \tag{22}$$

$$= \frac{2}{T}\int_{-\infty}^{+\infty} dt\Pi\left(\frac{\tau-t}{T}\right)\left[\mathcal{B}_\varphi(-t\vec{V}) - \mathcal{B}_\varphi(\vec{B}-t\vec{V})\right] \tag{23}$$

$$= \frac{1}{T}\int_{-\infty}^{+\infty} dt\Pi\left(\frac{\tau-t}{T}\right)\left[\mathcal{D}_\varphi(\vec{B}-t\vec{V}) - \mathcal{D}_\varphi(-t\vec{V})\right] \tag{24}$$

where we make use of the Taylor hypothesis to assume $\mathcal{B}_\varphi(\vec{B},t) = \mathcal{B}_\varphi(\vec{B}-t\vec{V})$.

We have now to determine the expression of $\mathcal{D}_{\varphi_T}(\vec{r},t)$ which is an estimation of $\mathcal{D}_{\varphi}(\vec{r},t)$ for a finite exposure time. In the case of finite exposure time, the time averaging acts like a low–pass filter[22] . The attenuation of high frequency components of phase fluctuations will lead to an underestimation of $\mathcal{D}_{\varphi}(\vec{r},t)$.

To obtain $\mathcal{D}_{\varphi_T}(\vec{r},t)$, we derive first the spatio–temporal correlation $\mathcal{B}_{\varphi_T}(\vec{B},\tau)$ of the phase fluctuations φ_T averaged for an exposure time T,

$$\mathcal{B}_{\varphi_T}(\vec{B},\tau) = \left\langle \left[\frac{1}{T}\varphi(\vec{r},t) * \Pi\left(\frac{t}{T}\right)\right] \overline{\left[\frac{1}{T}\varphi(\vec{r}+\vec{B},t+\tau) * \Pi\left(\frac{t+\tau}{T}\right)\right]} \right\rangle \tag{25}$$

where $*$ and $\bar{}$ stand for the convolution and the complex conjugate, respectively and $\Pi\left(t\right)$ is the rectangle function. Equation (25) can be easily rewritten

$$\mathcal{B}_{\varphi_T}(\vec{B},\tau) = \frac{1}{T}\mathcal{B}_{\varphi}(\vec{B},\tau) * \Lambda\left(\frac{\tau}{T}\right) \tag{26}$$

where $\mathcal{B}_{\varphi}(\vec{B},\tau)$ is the spatio-temporal correlation of the instantaneous phase and $\Lambda\left(\tau\right)$ is the triangle function[21]:

$$\begin{aligned} \Lambda\left(\frac{\tau}{T}\right) &= 1-\left|\frac{t}{T}\right|, \text{ if} \left|\frac{\mathrm{t}}{\mathrm{T}}\right| \leq 1 \\ &= 0, \text{ otherwise.} \end{aligned} \tag{27}$$

For $\tau = 0$, Equation (26) gives

$$\mathcal{B}_{\varphi_T}(\vec{B},0) = \mathcal{B}_{\varphi_T}(\vec{B}) = \frac{1}{T}\int_{-\infty}^{+\infty} du \mathcal{B}_{\varphi}(\vec{B},u)\Lambda\left(\frac{u}{T}\right) = \frac{1}{T}\int_{-\infty}^{+\infty} du \mathcal{B}_{\varphi}(\vec{B}-u\vec{V})\Lambda\left(\frac{u}{T}\right) \tag{28}$$

where we make use of the Taylor hypothesis to assume $\mathcal{B}_{\varphi}(\vec{B},u) = \mathcal{B}_{\varphi}(\vec{B}-u\vec{V})$. $\mathcal{D}_{\varphi_T}(\vec{r},t)$ is deduced from Equation (28) by the relation :

$$\mathcal{D}_{\varphi_T}(\vec{B}) = 2\left[\mathcal{B}_{\varphi_T}(0) - \mathcal{B}_{\varphi_T}(\vec{B})\right] \tag{29}$$

$$= \frac{2}{T}\int_{-\infty}^{+\infty} du \Lambda\left(\frac{u}{T}\right)\left[\mathcal{B}_{\varphi}(-u\vec{V}) - \mathcal{B}_{\varphi}(\vec{B}-u\vec{V})\right] \tag{30}$$

$$= \frac{1}{T}\int_{-\infty}^{+\infty} du \Lambda\left(\frac{u}{T}\right)\left[\mathcal{D}_{\varphi}(\vec{B}-u\vec{V}) - \mathcal{D}_{\varphi}(-u\vec{V})\right] \tag{31}$$

The OPD measured for an exposure time T is given by Eq. (3) where the structure function is given by Eq. (29). The error Υ_{OPD} between the instantaneous OPD and the averaged OPD is

$$\Upsilon_{OPD} = \frac{OPD(0) - OPD(T)}{OPD(0)} \ . \tag{32}$$

Finally, the structure function of the residual phase $\mathcal{D}_{\varphi_r}(\vec{B})$ is

$$\begin{aligned} \mathcal{D}_{\varphi_r}(\vec{B}) &= \mathcal{D}_{\varphi}(\vec{B}) + \frac{1}{T}\int_{-\infty}^{+\infty} dt \Lambda\left(\frac{t}{T}\right)\left[\mathcal{D}_{\varphi}(\vec{B}-t\vec{V}) - \mathcal{D}_{\varphi}(-t\vec{V})\right] \\ &\quad -\frac{2}{T}\int_{-\infty}^{+\infty} dt \Pi\left(\frac{\tau-t}{T}\right)\left[\mathcal{D}_{\varphi}(\vec{B}-t\vec{V}) - \mathcal{D}_{\varphi}(-t\vec{V})\right] \end{aligned} \tag{33}$$

$$= \mathcal{D}_{\varphi}(\vec{B}) + \frac{1}{T}\int_{-\infty}^{+\infty} dt \left[\Lambda\left(\frac{t}{T}\right) - 2\Pi\left(\frac{\tau-t}{T}\right)\right]\left[\mathcal{D}_{\varphi}(\vec{B}-t\vec{V}) - \mathcal{D}_{\varphi}(-t\vec{V})\right] \ , \tag{34}$$

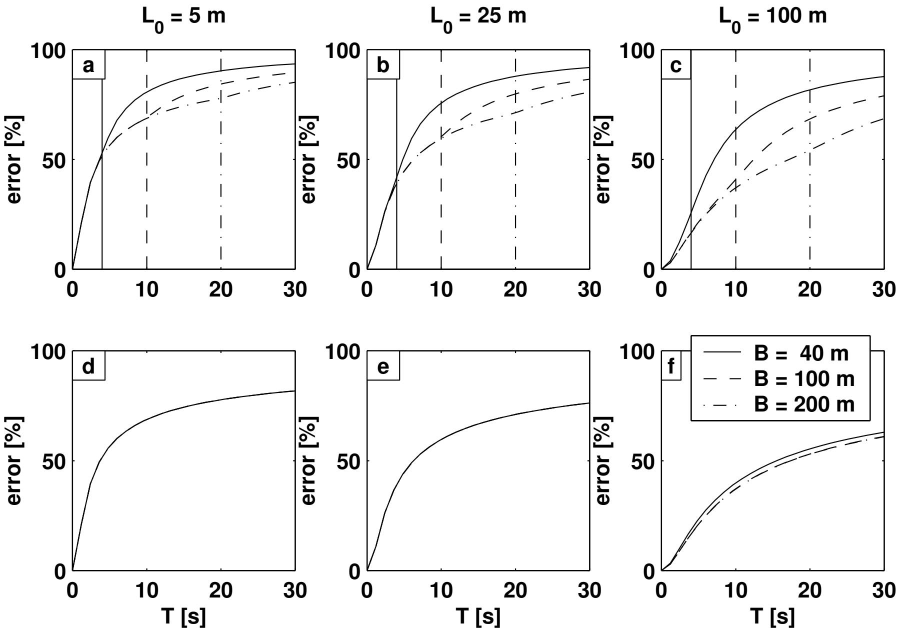

Figure 6. Υ_{OPD} versus T for different values of $\mathcal{L}_0$ and of the baseline B. The wind speed is equal to 10m.s^{-1} and the wind direction is parallel to the baseline for graphs a, b and c and perpendicular for graphs d, e and f. The diameter D is equal to 10m and r_0 is equal to 10cm. Vertical lines show the time B/V taken by turbulent eddies carried by the wind to cross the distance B between both telescopes.

Table 1. Variation of Υ_{OPD} with different parameters. $\nearrow$ means that Υ_{OPD} increases when the parameter increases and $\searrow$ means that Υ_{OPD} decreases when the parameter increases

Parameters $\nearrow$	T	$\mathcal{L}_0$	B	D	V	$\arg(\vec{V})$
Υ_{OPD}	$\nearrow$	$\searrow$	$\searrow$	$\searrow$	$\nearrow$	$\searrow$

and the residual OPD is deduced from Eq. (3).

Examples of the variations of Υ_{OPD} and of the residual OPD with the exposure time are given in Figs. (6) and (7) respectively, for different values of $\mathcal{L}_0$, B and $\arg(\vec{V})$ and for D, r_0 and V equal to 10m, 10cm and 10m.s^{-1}, respectively.

Tables 1 and 2 summarize the variation of Υ_{OPD} and of the residual OPD, respectively, for the parameters T, τ, r_0, $\mathcal{L}_0$, B, D, V and $\arg(\vec{V})$ when the value of each parameter is increased.

3. CONCLUSION

For the first time, a set of continuous nights of outer scale measurements has been undertaken at Paranal by the GSM. The mean value of $\mathcal{L}_0$ is 24 m and the log–statistics of $\mathcal{L}_0$ shows that the range [15m–37m] contains 68% of the $\mathcal{L}_0$ values measured at Paranal.

The exact formulation of the structure function of the phase fluctuations is derived for both cases with and without the filtering effect of an aperture of diameter D. These expressions directly related to the standard deviation of the OPD show that for baselines larger than $\mathcal{L}_0$, the OPD becomes independent of baseline values. It has been found that, at Paranal, for the diameter of one U.T. (8.2m), for baseline values typical for the VLTI (40m, 100m, 200m) and with the r_0 and $\mathcal{L}_0$ values measured by the GSM, the OPD is reduced by a factor 10 compared to a model with an infinite outer scale (Kolmogorov model). Moreover, the effect of baseline values on OPD value can be neglected.

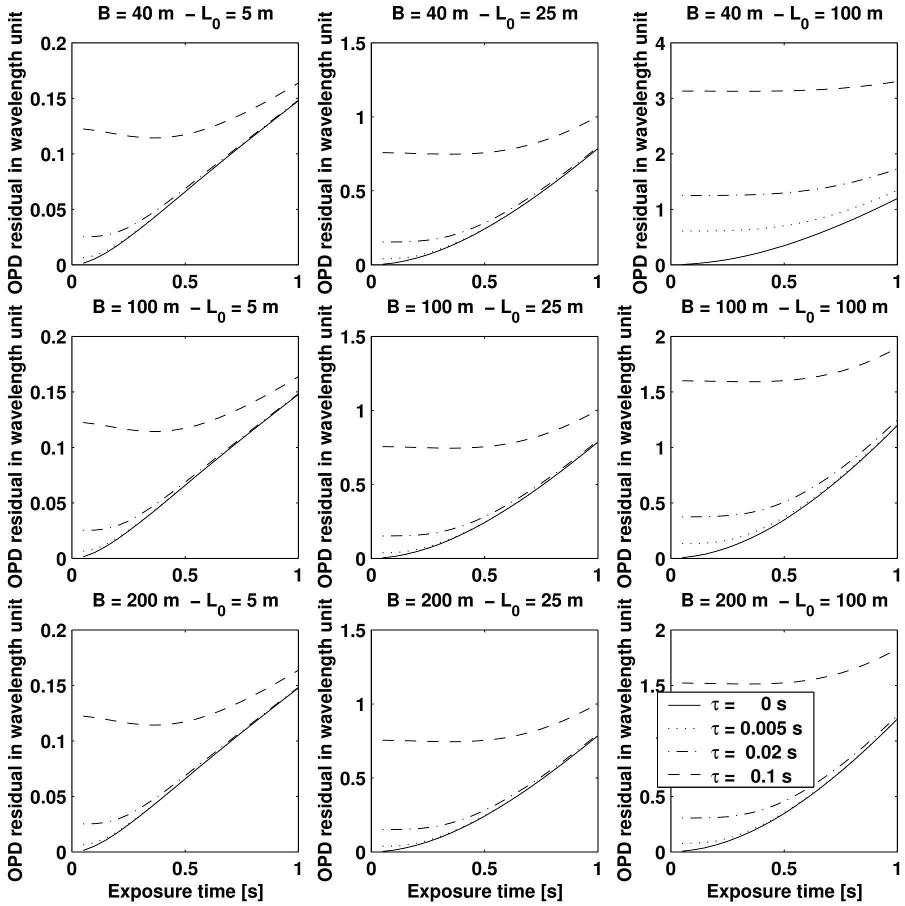

Figure 7. Residual OPD plotted as a function of the exposure time T for different values of $\mathcal{L}_0$: 5, 25 and 100 m from the left to the right, of B : 40, 100 and 200 m from the top to the bottom and of τ : 0ms(full line), 5ms(dotted line), 20ms(dotted–dashed line) and 100ms(dashed line). D, V and r_0 are equal to 10m, 10m.s^{-1} and 10cm, respectively and the wind direction is perpendicular to the baselines.

Table 2. Variation of the residual OPD with different parameters. $\nearrow$ means that the residual OPD increases when the parameter increases and $\searrow$ means that Υ_{OPD} decreases when the parameter increases.

Parameters $\nearrow$	T	τ	r_0	$\mathcal{L}_0$	B	D	V	arg($\vec{V}$)
Residual OPD	$\nearrow$	$\nearrow$	$\searrow$	$\nearrow$	$\searrow$	$\nearrow$	$\nearrow$	$\searrow$

The expression of the residual OPD at the output of a fringe tracker system is also derived for two sources of error : the finite exposure time T of the fringe sensor and the finite frequency of the closed–loop of the system i.e. the finite response time τ of the servo–control. The finite size of $\mathcal{L}_0$ permits, for fixed values of T and τ, to diminish the residual OPD value or to increase T and τ values keeping the residual OPD below a critical value (Fig. 7 and Table 2).

Finally, we have seen the gain for the co–phasing of an interferometer if we take into account the outer scale and, consequently, the finite size of $\mathcal{L}_0$ should be considered for the design and the technical specifications of the new Optical Long Baseline Interferometers.

REFERENCES

1. F. Martin, A. Tokovinin, A. Ziad, R. Conan, J. Borgnino, R. Avila, A. Agabi, and M. Sarazin, "First statistical data on wave front outer scale at La Silla observatory from the G.S.M. instrument," *Astron. Astrophys.* **336**, pp. L49–L52, 1998.
2. A. Tokovinin, A. Ziad, F. Martin, R. Avila, J. Borgnino, R. Conan, and M. Sarazin, "Wavefront outer scale monitoring at La Silla," in *Adaptive Optical System Technologies*, *Proc. SPIE* **3353**, pp. 1155–1162, March 1998.
3. R. Avila, A. Ziad, J. Borgnino, F. Martin, A. Agabi, and A. Tokovinin, "Theoretical spatio-temporal analysis of angle of arrival induced by atmospheric turbulence as observed with the Grating Scale Monitor experiment," *J. Opt. Soc. Am. A* **14**, pp. 3070–3082, November 1997.
4. C. Gardner, "Effects of random path fluctuations on the accuracy of laser ranging systems," *Applied Optics* **15**, pp. 2539–2545, October 1976.
5. R. Lutomirski and H. Yura, "Wave structure function and mutual coherence function of an optical wave in a turbulent atmosphere," *J. Opt. Soc. Am.* **61**(4), pp. 482–486, 1971.
6. G. Reinhardt and S. Collins, "Outer-scale effects in turbulence-degraded light-beam spectra," *J. Opt. Soc. Am.* **62**, pp. 1526–1528, December 1972.
7. F. Martin, R. Conan, A. Tokovinin, A. Agabi, J. Borgnino, A. Ziad, and M. Sarazin, "Report on the GSM measurement campaign at the Paranal observatory," ESO report VLT-TRE-UNI-17440-0006, ESO, 1998.
8. F. Martin, A. Tokovinin, A. Ziad, R. Conan, J. Borgnino, and R. Avila, "Report on G.S.M. measurement campaign at La Silla," ESO report VLT–TRE–UNI–17440–0005, ESO, 1998.
9. A. Tokovinin, V. Kornilov, R. Conan, A. Ziad, F. Martin, S. Ilyasov, S. Ehgamberdiev, Y. Tillaev, K. Sultanov, and M. Sarazin, "Report on the Maydanak site testing campaign in July 1998," Progress report N1, INTAS–96-0367, 1998.
10. D. Fried, "Optical resolution through a randomly inhomogeneous medium for very long and very short exposures," *J. Opt. Soc. Am.* **56**, pp. 1372–1379, October 1966.
11. F. Roddier, "The effect of atmospheric turbulence in optical astronomy," in *Progress in Optics*, vol. XIX, E. Wolf, 1981.
12. V. Tatarski, *Wave Propagation in a Turbulent Medium*, Dover Publications, Inc., New York, 1961.
13. M. Roggeman, B. Welsh, D. Montera, and T. Rhoadarmer, "Method for simulating atmospheric turbulence phase effects for multiple time slices and anisoplanatic conditions," *Applied Optics* **34**, pp. 4037–4051, July 1995.
14. G. Valley, "Long– and short–term Strehl ratios for turbulence with finite inner and outer scales," *Applied Optics* **18**, pp. 984–987, April 1979.
15. R. Sasiela, *Electromagnetic Wave Propagation in Turbulence. Evaluation and Application of Mellin Transforms*, Springer–Verlag, New–York, 1994.
16. J. Mariotti, "Adaptive optics for long baseline optical interferometry," in *Adaptive Optics for Astronomy*, D. Alloin and J.-M. Mariotti, eds., pp. 309–320, Kluwer Academic Publisher, 1994.
17. M. Shao, M. Colavita, B. Hines, D. Staelin, D. Hutter, K. Johnston, D. Mozurkewich, R. Simon, J. Hershey, J. Hughes, and G. Kaplan, "The mark III stellar interferometer," *Astron. Astrophys.* **193**, pp. 357–371, 1988.
18. J. Davis, P. Lawson, A. Booth, W. Tango, and E. Thorvaldson, "Atmospheric path variations for baselines up to 80 m measured with the Sydney University Stellar Interferometer," *Mon. Not. R. astr. Soc.* **273**, pp. L53–L58, 1995.
19. J. Armstrong, D. Mozurkewich, L. Rickard, D. Hutter, J. Benson, P. Bowers, N. Elias II, C. Hummel, K. Johnston, D. Buscher, J. Clark III, L. Ha, L.-C. Ling, N. White, and R. Simon, "The Navy Prototype Optical Interferometer," *Astrophysical Journal* **496**, pp. 550–571, March 1998.
20. M. Colavita, J. Wallace, B. Hines, Y. Gursel, F. Malbet, D. Palmer, X. Pan, M. Shao, J. Yu, A. Boden, P. Dumont, J. Gubler, C. Koresko, S. Kulkarni, B. Lane, D. Mobley, and G. V. Belle, "The Palomar Testbed Interferometer," *Astrophysical Journal* **510**, pp. 505–521, January 1999.
21. R. Bracewell, *The Fourier Transform and its Applications*, McGraw-Hill Book Company, New–York, 1978.
22. H. Martin, "Image motion as a measure of seeing quality," *JASP* **99**, pp. 1360–1370, December 1987.